

DYNAMIC INTERACTIONS OF MIXED FLUID COSMOLOGICAL MODELS IN MODIFIED GRAVITY

M. S. Palaspagar¹  and P. P. Khade² 

¹Department of Mathematics, Rajarshee Shahi Science College Chandur Rly. Di.Amravati, 444904, India

²Department of Mathematics, Vidya Bharati Mahavidyalaya Camp Amravati 444601, India

E-mail: mathsvbmvpk@gmail.com

(Received: December 29, 2024; Accepted: September 8, 2025)

SUMMARY: This study explores a Kantowski-Sachs cosmological model within the framework of Modified gravity, utilizing an interacting field as the energy source. The interacting field comprises a linear combination of electromagnetic, massless scalar, and charged perfect fluid components. Our analysis encompasses four distinct scenarios: perfect fluid, disordered radiation, dust fluid, and dark energy. By establishing a relationship between metric potentials, we solved the field equations and investigated pressure and density profiles using the equation of state. A comprehensive examination of cosmological and dynamical parameters was also conducted.

Key words. Cosmology: dark energy – Cosmology: theory – Cosmology: cosmological parameters – Gravitation

1. INTRODUCTION

The accelerating expansion of the universe remains a topic of great interest. Observations of Type Ia supernovae have consistently shown that the universe's expansion is accelerating (Perlmutter et al. 1997, Riess et al. 1998, Perlmutter et al. 1998, 1999, Spergel et al. 2003). To explain this phenomenon, researchers (Planck Collaboration et al. 2016, 2020) have proposed the existence of dark energy, a mysterious energy component with repulsive properties. Dark energy can be characterized using the equation of state parameter (EOS) $\omega = p/\rho$, where p is pressure and ρ is energy density.

Modified gravity theories, such as $f(R)$, $f(T)$ and $f(R, T)$ have been developed to explore dark energy and other cosmological issues. These theories provide a framework for understanding the universe's

accelerated expansion. For instance, the $f(R)$ theory naturally accounts for both the early-time inflation and late-time acceleration. Alternative theories, including the scalar-Gauss-Bonnet gravity ($f(G)$) and $f(T)$ gravity, have also been proposed to explain the accelerating universe.

A more generalized theory, the $f(R, T)$ gravity, has been introduced by (Harko and Lobo 2010, Harko et al. 2011), which incorporates an arbitrary function of the scalar curvature R and the trace of the energy-momentum tensor T . This theory has been explored extensively to address various cosmological issues. Researchers have explored various cosmological models within the $f(R, T)$ theory of gravity. For instance, Pawar et al. (2018a) derived a Kaluza-Klein string cosmological model, while Houndjo (2012) developed a cosmological scenario discussing a transition from a matter-dominated era. Tiwari et al. (2021) examined the LRS Bianchi type-I model with a variable deceleration parameter dependent on the Hubble parameter. Other studies (Santhi Kumar and Satyanarayana 2017, Santos 2013, Tretyakov 2018) have investigated accelerating anisotropic cosmological mod-

els, Gödel universe solutions, and cosmology in modified $f(R, T)$ gravity.

Recent studies (Tiwari et al. 2023, Bhardwaj and Rana 2019, Khade 2023, Tiwari and Sofuoğlu 2020) have also explored specific models, including the Bianchi type-I model with a decaying cosmological term, transition models via observational constraints, and LRS Bianchi-I transit universe with periodic varying q . Additionally, researchers have investigated the behavior of Bianchi Type-V dark energy models and quadratically varying deceleration parameters within this modified theory.

Researchers (Pawar et al. 2018b, Kandalkar et al. 2009, Reddy et al. 2014, Samanta 2013) have extensively explored Kantowski-Sachs cosmological models in various modified gravity theories. For instance, studies have examined tilted Kantowski-Sachs models in Brans-Dicke theory, viscous fluid models with varying Λ , and bulk viscous string cosmological models in $f(R, T)$ gravity.

Other investigations (Katore and Hatkar 2016, Santhi et al. 2016, Vinutha et al. 2023, Zubair and Ali Hassan 2016) have focused on Kantowski-Sachs universes filled with perfect fluid in the $f(R, T)$ theory, domain wall cosmological models, and scalar field cosmological models in modified gravity. The dynamics of Bianchi type I, III, and Kantowski-Sachs solutions in $f(R, T)$ gravity have also been explored.

Additionally, researchers (Singh et al. 2015, Sharif and Nawazish 2017, Rao et al. 2023) have analyzed bounce conditions in Kantowski-Sachs and Bianchi cosmologies, cosmological analysis of scalar field models, and dynamics of cosmological models with domain walls and massive scalar fields in $f(R, T)$ gravity.

Recent studies (Motavalli et al. 2016, Qazi et al. 2022, Amir and Yussouf 2015, Ghate and Sontakke 2018) have also investigated Kantowski-Sachs cosmological solutions in generalized teleparallel gravity, classification of Kantowski-Sachs and Bianchi type III solutions in $f(T)$ gravity, and ghost dark energy cosmological models with specific Hubble parameters in $f(R, T)$ gravity. This study investigates a Kantowski-Sachs cosmological model within the framework of $f(R, T)$ modified gravity. In this theory, the gravitational Lagrangian is an arbitrary function of the Ricci scalar R and the trace of the stress-energy momentum tensor T , taking the form $f(R, T) = R + 2f(T)$. The theoretical foundations of $f(R, T)$ gravity and the corresponding metric field equations are outlined in Section 2. Section 3 presents the derived solutions, while Section 4 discusses the dynamical properties of the model. Finally, Section 5 summarizes and concludes the findings.

2. METRIC AND FIELD EQUATIONS

Homogeneous and Anisotropic Kantowski-Sachs spacetime is:

$$ds^2 = dt^2 - A^2 dr^2 - B^2(d\theta^2 + \sin^2\theta d\phi^2), \quad (1)$$

where A and B are functions of cosmic time t .

Field Equations of the formalism of Hilbert-Einstein Variational Principle in $f(R, T)$ Gravity is:

$$S = \frac{1}{2} \int f(R, T) \sqrt{-g} d^4x + \int L_m \sqrt{-g} d^4x, \quad (2)$$

where the symbols have their usual meanings.

The gravitational field equations for $f(R, T)$ gravity is given by:

$$\begin{aligned} f_R(R, T)R_{ij} - \frac{1}{2}f(R, T)g_{ij} \\ + (g_{ij}\nabla^k\nabla_k - \nabla_i\nabla_j)f_R(R, T) \\ = (k - f_T(R, T))\bar{T}_{ij} - f_T(R, T)\theta_{ij}, \end{aligned} \quad (3)$$

where $\theta_{ij} = g^{\alpha\beta}\frac{\partial T_{\alpha\beta}}{\partial g^{ij}}$, $f_R = \frac{\partial f(R, T)}{\partial R}$, $f_T = \frac{\partial f(R, T)}{\partial T}$, ∇_i is the covariant derivative. We choose $k = \frac{8\pi G}{c^4}$, where G is the Newtonian Gravitational constant and c is speed of light in vacuum. \bar{T}_{ij} is the standard matter energy-momentum tensor derived from the Lagrangian L_m . We choose the matter Lagrangian only for a perfect fluid distribution as $L_m = -p$. We assumed the model:

$$f(R, T) = R + 2f(T), \quad (4)$$

where $f(T)$ is an arbitrary function of the trace of energy-momentum tensor and we choose $f(T) = \lambda T$ with λ taken as a constant. Now, the relativistic field equations of the $f(R, T)$ gravity theory for linearly coupled charged perfect fluid, source-free electromagnetic field, and mass-less scalar fields are:

$$G_{ij} = R_{ij} - \frac{1}{2}Rg_{ij} = (k + 2\lambda)\bar{T}_{ij} + \lambda(\bar{T} + 2p)g_{ij}. \quad (5)$$

Also, the Einstein field equation for general theory of relativity is given by:

$$G_{ij} = R_{ij} - \frac{1}{2}Rg_{ij} - \Lambda g_{ij} = -8\pi T_{ij}. \quad (6)$$

Here, Λ is the cosmological constant, which we use as the dark energy source. Comparing Eq. (5) with the Einstein field Eq. (6), we have:

$$\Lambda = \lambda(\bar{T} + 2p). \quad (7)$$

We considered the source of energy of the gravitational field as interacting field with dark energy and observed the behavior of the cosmological model in presence of linearly coupled perfect fluid distribution, mass-less scalar field, and source of a free electromagnetic field. That is:

$$\bar{T}_{ij} = S_{ij} + T_{ij} + E_{ij}, \quad (8)$$

where S_{ij} is the energy-momentum tensor for perfect fluid distribution and it is given by:

$$S_{ij} = (p + \rho)u_i u_j - g_{ij}p, \quad (9)$$

with

$$g^{ij}u_iu_j = 1, \quad (10)$$

where, p , ρ and u^i are internal pressure, rest mass density, and four-velocity vectors of the distribution, respectively. T_{ij} is the energy-momentum tensor for the mass-less scalar field and it is given by:

$$T_{ij} = U_{,i}U_{,j} - \frac{1}{2}g_{ij}U_sU^{',s}. \quad (11)$$

The mass-less scalar field U also satisfies

$$g^{ij}U_{;ij} = \rho_c, \quad (12)$$

where, ρ_c is the charge density, semicolon (;) and comma (,) denote the covariant derivative and partial derivative, respectively. E_{ij} is the electromagnetic energy-momentum tensor given by:

$$E_{ij} = \frac{1}{4\pi}[F_{i\alpha}F_j^\alpha - \frac{1}{4}g_{ij}F_{\alpha\beta}F^{\alpha\beta}]. \quad (13)$$

Here, F_{ij} is the electromagnetic field tensor obtained from the four potential ϕ_i :

$$F_{ij} = \phi_{i,j} - \phi_{j,i}, \quad (14)$$

$$F_{;j}^{ij} = -4\pi\rho_c u^i. \quad (15)$$

In the co-moving transformation system the magnetic field is considered along the z - axis only; therefore the non-vanishing components of electromagnetic fields F_{ij} are only F_{12} and F_{21} . Also, we have the electromagnetic field tensor anti-symmetric. The first set of Maxwell equations is:

$$F_{ij,k} + F_{jk,i} + F_{ki,j} = 0, \quad (16)$$

leading to:

$$F_{12} = M = \text{constant}. \quad (17)$$

Now, from Eqs. (8), (9), (13) for the metric Eq. (1), we have:

$$\bar{T} = -\dot{U}^2 - 3p + \rho. \quad (18)$$

Now, by using $F_{12} = \text{const.} = M$ and $u^4 \neq 0$, from Eq. (15) we have that the charge density is zero ($\rho_c = 0$).

The field equations of $f(R, T)$ Eq. (5), for the metric Eq. (1) can be expressed as:

$$2\frac{\ddot{B}}{B} + \frac{\dot{B}^2}{B^2} + \frac{1}{B^2} = -(k + 2\lambda)\left[\frac{M^2}{8\pi A^2 B^2} - \frac{\dot{U}^2}{2} - p\right] - \lambda[\rho - p - \dot{U}^2], \quad (19)$$

$$\frac{\ddot{A}}{A} + \frac{\ddot{B}}{B} + \frac{\dot{A}\dot{B}}{AB} = -(k + 2\lambda)\left[\frac{M^2}{8\pi A^2 B^2} - \frac{\dot{U}^2}{2} - p\right] - \lambda[\rho - p - \dot{U}^2], \quad (20)$$

$$\frac{\ddot{A}}{A} + \frac{\ddot{B}}{B} + \frac{\dot{A}\dot{B}}{AB} = -(k + 2\lambda)\left[\frac{-M^2}{8\pi A^2 B^2 - \frac{\dot{U}^2}{2} - p}\right] - \lambda[\rho - p - \dot{U}^2], \quad (21)$$

$$2\frac{\dot{A}\dot{B}}{AB} + \frac{\dot{B}^2}{B^2} + \frac{1}{B^2} = -(k + 2\lambda)\left[\frac{-M^2}{8\pi A^2 B^2} + \frac{\dot{U}^2}{2} + \rho\right] - \lambda[\rho - p - \dot{U}^2]. \quad (22)$$

From Eq. (5) and Eq. (11), we get:

$$\frac{\ddot{U}}{U} + \frac{\dot{A}}{A} + 2\frac{\dot{B}}{B} = 0. \quad (23)$$

Here the dot stands for differentiation with respect to time t .

3. SOLUTION OF THE FIELD EQUATIONS

The system of Eqs. (19) - (22) comprises the nonlinear differential equations with five unknowns: A , B , U , p , and ρ . To elucidate the physical properties of the universe described by Eq. (1), we seek to determine these variables. However, solving these equations directly is challenging. To obtain the exact solutions, we introduce additional constraints that facilitate the derivation of specific solutions for Eqs (19) - (22). We begin by establishing a relationship between the metric potentials, which enables us to simplify the field equations and extract meaningful physical insights.

$$A = B^n, n \neq 1. \quad (24)$$

From Eq. (24), the field Eqs (19) - (22) reduce to:

$$\frac{\ddot{B}}{B} + (1+n)\frac{\dot{B}^2}{B^2} + \frac{1}{(1-n)B^2} = 0. \quad (25)$$

The above equation can be written as:

$$\frac{df^2}{dB} + \frac{2(1+n)f^2}{B} = \frac{2}{(n-1)B}, \quad (26)$$

where, $\dot{B}' = f(B)$.

From Eq. (26), we get:

$$\frac{dB}{d\tau} = \left[\frac{1}{2(n^2-1)} + \frac{k_1}{B^{(2n+2)}}\right]^{1/2}, \quad (27)$$

where k_1 is the integration constant, and $\frac{d^2\tau}{dt^2} = -\frac{k(n+1)}{\tau^{2n+3}}$. After suitable coordinate transformations, we will explore the physical characteristics of dynamic parameters of the cosmological model described in Eq. (1) as:

$$ds^2 = \left[\frac{1}{2(n^2-1)} + \frac{k_1}{\tau^{(2n+2)}}\right]^{-1}d\tau^2 - \tau^n dr^2 - \tau^2(d\theta^2 + \sin^2\theta d\phi^2). \quad (28)$$

Within the framework of $f(R, T)$ gravity, we explored a Kantowski-Sachs cosmological model that incorporates interactions between a charged perfect fluid, massless scalar field, and source-free electromagnetic field. Our analysis of this model yielded

specific physical and dynamical parameters, as presented in Eq. (28), which provide valuable insights into the model's behavior. Hubble Parameter:

$$H = \frac{(n+2)}{3\tau} \left[\frac{1}{2(n^2-1)} + \frac{k_1}{\tau^{(2n+2)}} \right]^{1/2}, \quad (29)$$

scalar expansion and shear scalar:

$$\theta = \frac{(n+2)}{\tau} \left[\frac{1}{2(n^2-1)} + \frac{k_1}{\tau^{(2n+2)}} \right]^{1/2}, \quad (30)$$

$$\sigma^2 = \frac{2(n-1)^2}{3\tau^2} \left[\frac{1}{2(n^2-1)} + \frac{k_1}{\tau^{(2n+2)}} \right], \quad (31)$$

average scale factor:

$$a = \tau^{\frac{(n+2)}{3}}, \quad (32)$$

spatial volume:

$$V = \tau^{(n+2)}. \quad (33)$$

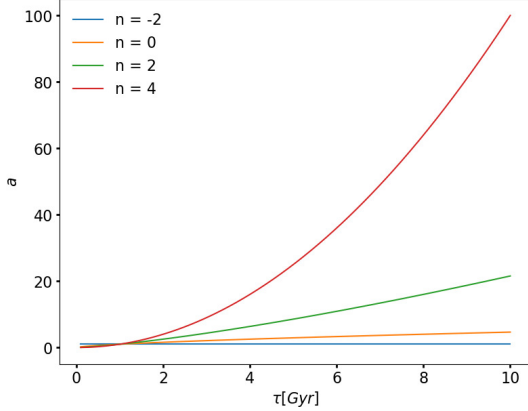


Fig. 1: Average scale factor (a) vs. cosmic time (τ) in Gyrs.

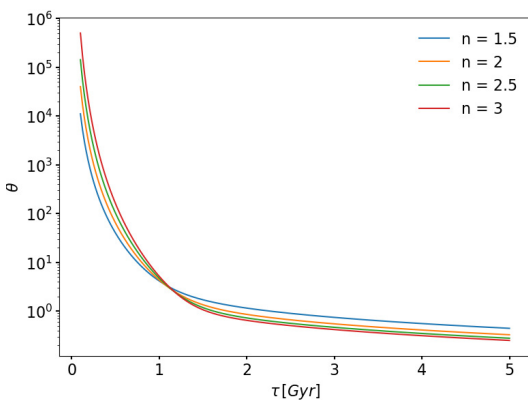


Fig. 2: Expansion scalar (θ) vs. cosmic time (τ) in Gyrs.

Average anisotropy parameter,

$$A_m = 2 \left[\frac{n-1}{n+2} \right]^2. \quad (34)$$

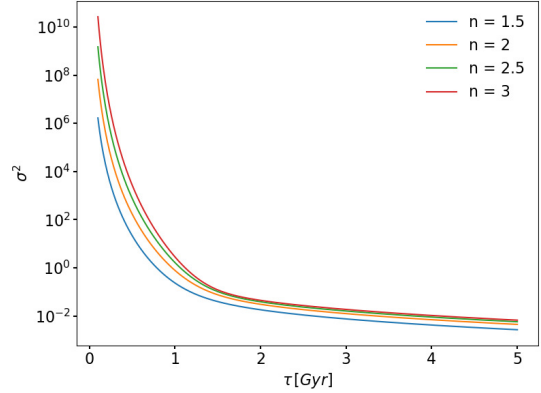


Fig. 3: Shear scalar (σ^2) vs. cosmic time (τ) in Gyrs.

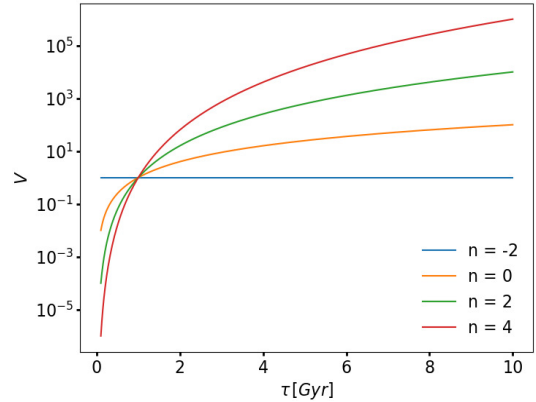


Fig. 4: Spatial volume (V) vs. cosmic time (τ) in Gyrs.

The deceleration parameter:

$$q = -1 + \frac{3}{2(n+2)} \left[\frac{1}{(n^2-1)} + \frac{2k_1(n+2)}{\tau^{(2n+2)}} \right] \times \left[\frac{1}{2(n^2-1)} + \frac{k_1}{\tau^{(2n+2)}} \right]^{-1}. \quad (35)$$

The evolution of the average scale factor is depicted in Fig. 1, which reveals a divergence in finite time. Notably, the scale factor's behavior is consistent across various values of n in this model. Fig. 2 illustrates the Hubble parameter's decrease over time.

The expansion and shear scalars exhibit divergent behavior at the initial epoch, as evident in Figs. 2 and 3. Eq. (30) indicates that the expansion scalar is infinite at $T = 0$, suggesting a point-type singularity at the initial epoch. This implies that the universe begins with a negligible volume and infinite expansion rate.

Fig. 3 shows that the shear scalar is positive, decreasing over time, and converges to zero as τ approaches infinity. The spatial volume, as seen in Fig. 4, increases with time, indicating an expanding universe. Fig. 5 illustrates deceleration of parame-

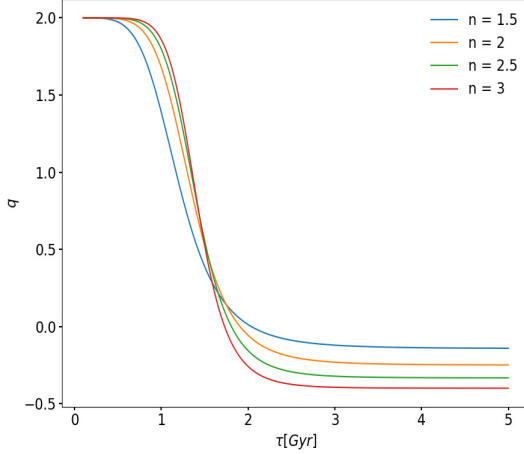


Fig. 5: Deceleration parameter (q) vs. cosmic time (τ) in Gyrs.

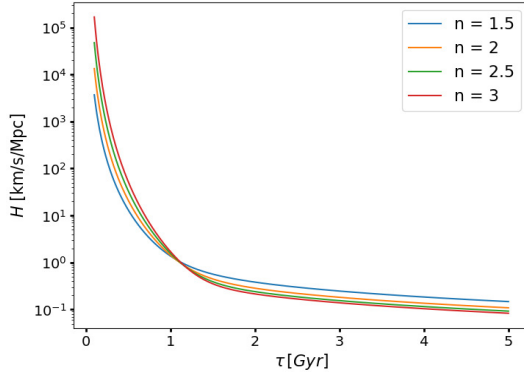


Fig. 6: Hubble parameter (H) in km/s/Mpc vs. cosmic time (τ) in Gyrs.

ter's transition from positive to negative values over time, eventually approaching -1 as τ approaches infinity.

Our cosmological model exhibits a transition from an initial decelerating phase to the current accelerating phase. The anisotropy (A_m) remains constant, indicating anisotropic behavior throughout the universe's evolution.

Recent observational data from SNeIa and CMBR suggest accelerating models, with the present value of the deceleration parameter q_0 falling within the range $-1.27 < q < 2$. Our model shows consistency with observational values of the Hubble and deceleration parameters.

4. DYNAMICAL PROPERTIES OF THE MODEL

In Eq. (35), we derived an expression for the deceleration parameter, which exhibits both positive and negative values over a specific time interval for chosen constant values. This prompted us to explore exact solutions for pressure and density in both de-

celerating and accelerating universe scenarios across four distinct cases. To achieve this, we employed the equation of state, $\omega = p/\rho$, with specific ω values, in conjunction with the previously assumed relationship between metric potentials, as given in Eq. (24).

- $\omega = 1$, Zeldovich fluid or stiff fluid,
- $\omega = 1/3$, disordered radiation,
- $\omega = 0$, dust fluid and
- $\omega = -1$, dark energy.

4.1. Zeldovich Fluid Model

To find the precise solution to the field Eqs. (19) - (22), we employed the second constraint, which takes form of an equation of state for a stiff fluid. We have:

$$p = \rho. \quad (36)$$

Using Eq. (36) in Eq. (19), the pressure and density of the model (Eq. (28)) are:

$$p = \rho = \frac{1}{(k + 2\lambda)\tau^2} \left[1 + \frac{1}{2(n^2 - 1)} - \frac{k_1(2n + 1)}{\tau^{(2n+2)}} \right] - \left[\frac{k_2^2(k + 4\lambda)}{2(k + 2\lambda)\tau^{(2n+2)}} - \frac{M^2}{8\pi\tau^{2n+2}} \right]. \quad (37)$$

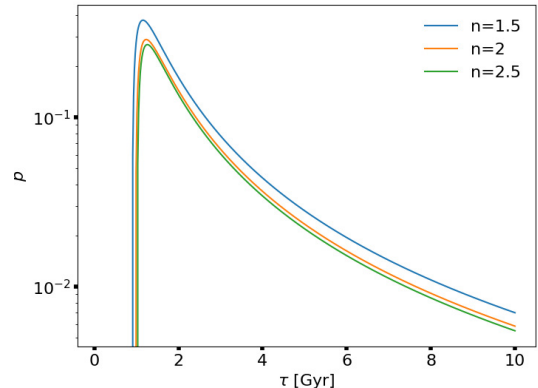


Fig. 7: Pressure (p) vs. cosmic time (τ) in Gyrs.

Upon examining Eq. (37), we notice that both the pressure and energy density of matter increase with time τ . Initially, the pressure assumes a small negative value, which grows as time progresses. A significant transition occurs at $\tau > 1.33$, where the pressure's sign changes from negative to positive. In the context of modern cosmology, the negative pressure is associated with accelerated expansion. Our analysis reveals that the universe undergoes an accelerated phase.

4.2. Dust Fluid Model

For a dust fluid, we have:

$$p = 0. \quad (38)$$

Using Eq. (38) in Eq. (19), the pressure and density of the model (Eq. (28)) becomes:

$$\begin{aligned} \rho = & \left[\frac{k_2^2(k+4\lambda)}{2\lambda\tau^{(2n+2)}} - \frac{M^2(k+2\lambda)}{8\pi\lambda\tau^{2n+2}} \right] \\ & - \frac{1}{\lambda\tau^2} \left[1 + \frac{1}{2(n^2-1)} - \frac{k_1(2n+1)}{\tau^{(2n+2)}} \right]. \end{aligned} \quad (39)$$

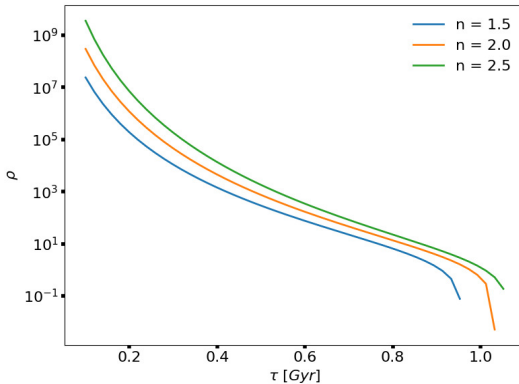


Fig. 8: Density (ρ) vs. cosmic time (τ) in Gyrs.

According to Eq. (39), the energy density exhibits large positive values at early times, gradually decreasing to zero at a certain point. Notably, the energy density then undergoes a sign change, transitioning from positive to negative values over time. Ultimately, it settles at a small negative value in the later stages of the universe's evolution.

4.3. Disordered Radiation Model

For disordered radiation EoS is:

$$\rho = 3p. \quad (40)$$

Using Eq. (40) in Eq. (19), the pressure and density of the model (Eq. (28)) yields:

$$\begin{aligned} p = & \frac{1}{k\tau^2} \left[1 + \frac{1}{2(n^2-1)} - \frac{k_1(2n+1)}{\tau^{(2n+2)}} \right] \\ & + \left[\frac{3M^2(k+2\lambda)}{8\pi k\tau^{2n+2}} - \frac{3k_2^2(k+4\lambda)}{2k\tau^{(2n+2)}} \right], \end{aligned} \quad (41)$$

$$\begin{aligned} \rho = & \frac{3}{k\tau^2} \left[1 + \frac{1}{2(n^2-1)} - \frac{k_1(2n+1)}{\tau^{(2n+2)}} \right] \\ & + \left[\frac{3M^2(k+2\lambda)}{8\pi k\tau^{2n+2}} - \frac{3k_2^2(k+4\lambda)}{2k\tau^{(2n+2)}} \right]. \end{aligned} \quad (42)$$

From Eq. (42) one can observe that the pressure and energy density are positive for $\tau > 1.33$ and they increase with time τ .

4.4. Dark Energy Model

For dark energy EoS parameter $\omega = -1$, we have

$$p = -\rho. \quad (43)$$

Using Eq. (43) in Eq. (19), the pressure and density of the model (Eq. (28)) become:

$$\begin{aligned} p = & \frac{1}{(k+4\lambda)\tau^2} \left[1 + \frac{1}{2(n^2-1)} - \frac{k_1(2n+1)}{\tau^{(2n+2)}} \right] \\ & + \left[\frac{M^2(k+2\lambda)}{8\pi(k+4\lambda)\tau^{2n+2}} - \frac{k_2^2}{2\tau^{(2n+2)}} \right], \end{aligned} \quad (44)$$

$$\begin{aligned} \rho = & -\frac{1}{(k+4\lambda)\tau^2} \left[1 + \frac{1}{2(n^2-1)} - \frac{k_1(2n+1)}{\tau^{(2n+2)}} \right] \\ & - \left[\frac{M^2(k+2\lambda)}{8\pi(k+4\lambda)\tau^{2n+2}} - \frac{k_2^2}{2\tau^{(2n+2)}} \right]. \end{aligned} \quad (45)$$

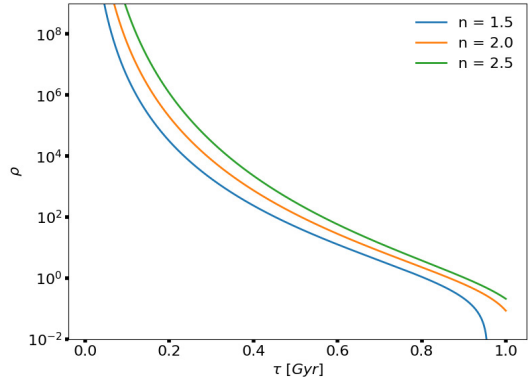


Fig. 9: Density (ρ) vs. cosmic time (τ) in Gyrs.

Fig. 9 illustrates the evolution of energy density ρ over time. Initially, ρ exhibits substantial positive values, which gradually decrease to zero at a specific point. Beyond this point, the energy density undergoes a sign reversal, transitioning from positive to negative values. Ultimately, it stabilizes at a relatively small negative value in the universe's later stages.

The pressure's behavior is also noteworthy. In the early universe, pressure assumes a negative value, but as time progresses, it increases and eventually approaches a positive constant value in later periods.

5. CONCLUSION

In this paper, we have considered a Kantowski-Sachs cosmological model within the framework of Modified gravity, utilizing an interacting field as the

energy source. We derived exact solutions to the field equations by assuming a relationship between the metric potentials. This study examines the evolution of a cosmological model, revealing a divergence in the average scale factor in finite time. The model exhibits a transition from initial decelerating phase to accelerating phase, consistent with recent observational data from SNeIa and CMBR. The key features include a point-type singularity at the initial epoch, an expanding spatial volume, and anisotropic behavior throughout the universe's evolution. The model's predictions for the Hubble and deceleration parameters align with observational values, supporting the validity of this cosmological framework. The deceleration parameter, is revealing its dynamic behavior across both decelerating and accelerating universe scenarios. By exploring the exact solutions for pressure and density across four distinct cases, we investigate the cosmological implications of varying equation of state parameters and metric potentials. Fig. 9 shows the evolution of energy density ρ over time, starting with positive values that decrease to zero and then further to negative values. The energy density stabilizes at a small negative value in the universe's later stages. In contrast, the pressure begins with a negative value in the early universe, increases over time, and approaches a positive constant value in later periods. This behavior is noteworthy and provides insight into the universe's evolution. The transition in energy density and pressure reflects the universe's dynamic behavior.

REFERENCES

Amir, M. J. and Yussouf, M. 2015, *International Journal of Theoretical Physics*, **54**, 2798

Bhardwaj, V. K. and Rana, M. K. 2019, *International Journal of Geometric Methods in Modern Physics*, **16**, 1950195

Ghate, H. R. and Sontakke, A.S. 2018, *Iranian Journal of Science and Technology, Transactions A: Science*, **42**, 847

Harko, T. and Lobo, F. S. N. 2010, *European Physical Journal C*, **70**, 373

Harko, T., Lobo, F. S. N., Nojiri, S. and Odintsov, S. D. 2011, *PhRvD*, **84**, 024020

Houndjo, M. J. S. 2012, *IJMPD*, **21**, 1250003

Kandalkar, S. P., Khade, P. P. and Gawande, S. P. 2009, *Turkish Journal of Physics*, **33**, 155

Katore, S. D. and Hatkar, S. P. 2016, *Progress of Theoretical and Experimental Physics*, **2016**, 033E01

Khade, P. P. 2023, *Jordan Journal of Physics*, **16**, 51

Motavalli, H., Akbarieh, A. R. and Nasiry, M. 2016, *MPLA*, **31**, 1650095

Pawar, D. D., Bhuttampalle, G. G. and Agrawal, P. K. 2018a, *NewA*, **65**, 1

Pawar, D. D., Shahare, S. P. and Dagwal, V. J. 2018b, *MPLA*, **33**, 1850011

Perlmutter, S., Gabi, S., Goldhaber, G., et al. 1997, *ApJ*, **483**, 565

Perlmutter, S., Aldering, G., della Valle, M., et al. 1998, *Natur*, **391**, 51

Perlmutter, S., Aldering, G., Goldhaber, G., et al. 1999, *ApJ*, **517**, 565

Planck Collaboration, Ade, P. A. R., Aghanim, N., et al. 2016, *A&A*, **594**, A13

Planck Collaboration, Aghanim, N., Akrami, Y., et al. 2020, *A&A*, **641**, A6

Qazi, S., Hussain, F., Ramzan, M. and Haq, S. 2022, *International Journal of Geometric Methods in Modern Physics*, **19**, 2250188

Rao, V. S., Ganesh, V. and Dasunaidu, K. 2023, *MPLA*, **38**, 2350093

Reddy, D. R. K., Anitha, S. and Umadevi, S. 2014, *European Physical Journal Plus*, **129**, 96

Riess, A. G., Filippenko, A. V., Challis, P., et al. 1998, *AJ*, **116**, 1009

Samanta, G. C. 2013, *International Journal of Theoretical Physics*, **52**, 2647

Santhi, M. V., Rao, V. U. M. and Aditya, Y. 2016, *Canadian Journal of Physics*, **95**, 718

Santhi Kumar, R. and Satyannarayana, B. 2017, *Indian Journal of Physics*, **91**, 1293

Santos, A. F. 2013, *MPLA*, **28**, 1350141

Sharif, M. and Nawazish, I. 2017, *European Physical Journal C*, **77**, 198

Singh, T., Chaubey, R. and Singh, A. 2015, *IJMPA*, **30**, 1550073

Spergel, D. N., Verde, L., Peiris, H. V., et al. 2003, *ApJS*, **148**, 175

Tiwari, R. K. and Sofuoğlu, D. 2020, *International Journal of Geometric Methods in Modern Physics*, **17**, 2030003

Tiwari, R. K., Mishra, S. K. and Sofuoğlu, D. 2021, *Journal of Applied Mathematics and Physics*, **9**, 847

Tiwari, R. K., Shukla, B. K., Sofuoğlu, D. and Kösem, D. 2023, *Symmetry*, **15**, 788

Tretyakov, P. V. 2018, *European Physical Journal C*, **78**, 896

Vinutha, T., Niharika, K. and Kavya, K. S. 2023, *Ap*, **66**, 64

Zubair, M. and Ali Hassan, S. M. 2016, *Ap&SS*, **361**, 149

ДИНАМИЧКЕ ИНТЕРАКЦИЈЕ КОД КОСМОЛОШКОГ МОДЕЛА МЕШОВИТИХ ФЛУИДА У МОДИФИКОВАНОЈ ГРАВИТАЦИЈИ

M. S. Palaspagar¹  and P. P. Khade² 

¹Department of Mathematics, Rajarshee Shahu Science College Chandur Rly. Di.Amravati, 444904, India

²Department of Mathematics, Vidya Bharati Mahavidyalaya Camp Amravati 444601, India

E-mail: mathsvbmvpk@gmail.com

УДК 524.83 : 530.12
Оригинални научни рад

Ова студија истражује космоловски модел Кантовски-Сакс (Kantowski-Sachs) у оквиру модификоване гравитације, користећи интерактивно поље као извор енергије. Интерактивно поље се састоји од линеарне комбинације електромагнетне, безмасене скаларне и наелектрисане компоненте идеалног флуида. Наша анализа обухвата четири различита слу-

чаја: идеални флуид, неуређено зрачење, прашинasti флуид и тамну енергију. Успостављањем везе између метричких потенцијала, решили смо једначине поља и истражили расподеле притиска и густине користећи једначину стања. Такође смо спровели свеобухватно испитивање космоловских и динамичких параметара.